/N-37
37984
p 24

High Temperature NASP Engine Seals
A Technology Review

Bruce M. Steinetz and Christopher DellaCorte
National Aeronautics and Space Administration
Lewis Research Center
Cleveland, Ohio

and

Mike Tong
Sverdrup Technology, Inc.
Lewis Research Center Group
Brook Park, Ohio

August 1991

NASA

HIGH TEMPERATURE NASP ENGINE SEALS:
A TECHNOLOGY REVIEW (U)

Progress in developing advanced high temperature engine seal concepts and related sealing technologies for advanced hypersonic engines are reviewed. Design attributes and issues requiring further development for both the ceramic wafer seal and the braided ceramic rope seal are examined. Leakage data are presented for these seals for engine simulated pressure and temperature conditions and compared to a target leakage limit. Basic elements of leakage flow models to predict leakage rates for each of these seals over the wide range of pressure and temperature conditions anticipated in the engine are also presented. The paper concludes with an outline of a seal development program to address the seal technology issues raised during the Technical Maturation Phase of the National Aerospace Plane Program.

NASP ENGINE PANEL SEALS (U)

NASA Lewis Research Center is developing advanced seal concepts and sealing technology for the NASP propulsion system. The majority of the development effort has been applied to maturing panel-edge seals that seal the many feet of sliding seal interfaces between the movable engine panels and stationary splitter walls. An example of the seals being developed is the ceramic wafer seal shown mounted in the movable nozzle panel, one of the many movable panels in the engine. The goal of the panel edge seals is to prevent hot engine flow path gases, flowing beneath the engine panels in the figure, from escaping through the seal systems and damaging engine panel support and articulation systems.

The objective of this paper is to summarize the major high temperature sealing technology accomplishments made during the Technical Maturation Program at NASA Lewis Research Center in the areas of seal concept development, high-temperature seal performance evaluation, seal leakage model formulation, and seal material friction and lubrication assessment. Plans to further mature these seal technologies over the next phase of the project under Government Work Package 79 will also be reviewed.
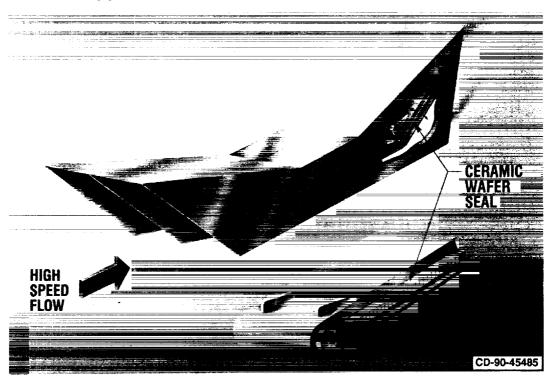
Hypersonic Engine Ceramic Wafer Seal

CERAMIC WAFER SEAL

HIGH SPEED FLOW

CD-90-45485

Figure 1.

SEAL CONCEPTS UNDER DEVELOPMENT (U)

Two seal designs that show promise of meeting the demanding operating conditions of the NASP engine environment and sealing the gaps between the movable horizontal panels and the vertical splitter walls are the ceramic wafer seal and the braided ceramic rope seal. The ceramic wafer seal developed by NASA Lewis Research Center (ref. 1) is constructed of multiple ceramic wafers mounted in a close tolerance horizontal channel along the side of the movable horizontal engine panel. The seal is preloaded against the engine splitter wall using an active preload approach such as a series of cooled pressurized metal bellows shown in the figure. The bellows push against a flexible metal backing plate that distributes the load to the wafers between the discrete circular bellows. The wafer seal conforms to expected engine splitter wall distortions by relative sliding between adjacent wafers. Leakage tests conducted at room- and high-temperatures at NASA Lewis Research Center have shown this design accommodates and seals both straight and simulated distorted walls as will be described later in this paper.

The braided ceramic rope seal is fabricated using either two- or three-dimensional braid architectures. Braiding the seal from alumina-boria-silicate (Nextel) fibers allows the seal to operate up to 2300 °F. Tests have shown (ref. 2) that these ceramic fibers maintain both strength and flexibility after exposure to this temperature. Several seal constructions based on braided rope seal technology are being considered for the engine depending on engine location and local heating rates. For the highest heating rate areas of the engine hollow braided rope seals pressurized from within are being considered. Using this approach the gas pressurization both inflates the seal conforming it to the expected engine wall distortion and transpires through the seal to effectively cool it. In less severe heating locations solid rope seals are being considered. These seals can be either mounted in close conforming seal channels or if required, can be preloaded with an active preload system such as the metal bellows shown.

Seal Concepts Under Development

CERAMIC WAFER SEAL

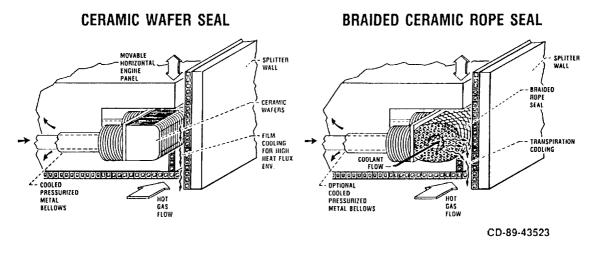### BRAIDED CERAMIC ROPE SEAL

CD-89-43523

Figure 2.

CERAMIC WAFER SEAL DESIGN CRITIQUE (U)

The ceramic wafer seal has several important features making it a strong contender for the NASP engine seals. Made of engineered ceramics, the seal can potentially operate to 2500 °F without coolant. High strength properties of modern engineered ceramics make them suitable for the pressure levels (up to 100 psi) anticipated in the NASP engine. The stacked arrangement of the ceramic wafers allows them to accommodate and seal straight and engine-simulated distorted walls. Thermal analyses conducted in references 3 and 4 and summarized later in this paper have shown that the wafer seal made of silicon carbide with high thermal conductivity can operate with only passive coolant (i.e., conduction into surrounding panels) to heat fluxes up to 300 Btu/ft^2sec. Furthermore, the analysis showed the seal could survive much higher heat fluxes (up to 1160 Btu/ft^2sec) typical of the combustor entrance region at Mach 10 flight condition using a small amount of film coolant. Besides these excellent technical advantages, the ceramic wafer seal design offers the practical advantage of fitting in the required envelope.

Issues that need to be addressed to fully mature the seal technology include: reducing the high friction typical of ceramics; verifying the durability and leakage rates over engine cycle life; and assessment of ceramic wafer seal response to the sudden thermal transients. To address the issue of cyclic durability, tests must be performed in which prototype seal specimens are scrubbed against candidate engine wall surfaces over the wide seal temperature range. To address the friction issue, NASA Lewis Research Center has begun a program to characterize baseline unlubricated ceramic friction coefficients and evaluate high temperature lubricants such as silver, gold, and PS-212 (a NASA Lewis Research Center developed lubricant, ref. 5). Some results from this program will be discussed later in this paper. Another important issue to be assessed is the ceramic wafer material resistance to sudden thermal transients anticipated in the engine. Recent tests were performed by Eckel, et al. (ref. 6) to rank the relative thermal-structural performance of selected ceramics subjected to intense heating rates of rocket engine exhaust gases. In these tests material samples were subjected to sudden direct impingement of the hot gas flow. Though some specimens failed, these test conditions are more severe than those anticipated for the tangentially mounted wafer seal. Tests are planned to subject the wafer seal materials to the more representative heating conditions of tangential flows which are less than a tenth those of the direct impingement case.

Ceramic Wafer Seal Design Critique

DESIGN ATTRIBUTES:
— HIGH TEMPERATURE, HIGH-PRESSURE OPERATION
— LOW LEAKAGE: SEALS STRAIGHT AND DISTORTED ENGINE WALLS
— HIGH HEAT FLUX OPERATION

PASSIVE COOLANT: UP TO 300 Btu/ft^2 s

ACTIVE COOLANT: UP TO 1160 Btu/ft^2 s

— OFF-THE-SHELF TECHNOLOGY
— COMPACT PACKAGING

ISSUES FOR FURTHER DEVELOPMENT/(OPTIONS):
— HIGH FRICTION COEFFICIENTS (SOLID FILM LUBRICANTS)

— MAINTAINED LOW LEAKAGE OVER REPEATED CYCLING
  (SEAL SCRUBBING TESTS/ DEVELOPMENT)

— MATERIAL RESISTANCE TO THERMAL TRANSIENTS
  (THERMAL TESTS AND DEVELOPMENT)

Figure 3.

BRAIDED CERAMIC ROPE SEAL CRITIQUE (U)

Features making the braided ceramic rope seal a strong engine seal candidate include: the seal's excellent conformability; the potential for high temperature, high pressure operation; and the design's excellent adaptability to seal ill-defined or complicated locations such as corners, hinge lines and other areas. The seal packages well within the limited design envelope and can easily be adapted to other locations on the NASP vehicle.

There are several important issues that must be addressed and traded-off against one another to fully mature this seal technology. Passive cooling of the braided ceramic rope design is limited by two important factors: (1) the fibers in a braided architecture have limited thermal conduction paths through the thickness of the rope, and (2) the thermal conductivity of alumina-boria-silicate fibers is quite small. These conditions taken together give the braided ceramic rope a very low through-the-thickness conductivity. Since the rope acts as an insulator the outer fibers of the seal get hot and reach the operating temperature limit at low heat flux rates. Calculations performed at NASA Lewis Research Center and corroborated by Boeing Advanced Systems (ref. 7) show that the maximum heat flux the braided rope design could operate to with only passive coolant (i.e., conduction into adjacent panels) is of the order of 20 Btu/ft^2sec. At higher heat fluxes typical of the NASP engine, significant flow rates of active coolant are required to maintain the outer fibers of the rope seal within their operating limit.

Other issues that are being addressed include development of low permeability braided structures that meet the leakage limits established and minimize "overcooling" of the transpiration cooled seal design. A considerable amount of progress has recently been made in reducing braid permeability as will be described later in this paper. Also crucial to the successful development of this seal concept is fabrication of braid structures that maintain their low permeability over repeated cycling in the engine, which is a main goal of work to be pursued under Government Work Package 79 at NASA Lewis Research Center.

Braided Ceramic Rope Seal Design Critique

DESIGN ATTRIBUTES:
— HIGH TEMPERATURE, HIGH-PRESSURE OPERATION
— EXCELLENT CONFORMABILITY TO DISTORTED ENGINE WALLS
— SEALS CORNERS AND HINGELINES
— ADAPTABLE TO OTHER VEHICLE LOCATIONS
— COMPACT PACKAGING

ISSUES FOR FURTHER DEVELOPMENT/(OPTIONS):
— LOW THROUGH-THE-THICKNESS CONDUCTIVITY LIMITS PASSIVELY
   COOLED HEAT FLUXES TO 20 $Btu/ft^2 s$ (HIGH COOLANT FLOW RATES)

— LOW PERMEABILITY BRAID REQUIRED
   (OPTIMIZED SEAL BRAID ARCHITECTURES)

— MAINTAINING REQUIRED PERMEABILITY OVER REPEATED CYCLING
   (COMBINED SEAL SCRUBBING/PERMEABILITY TESTS AND DEVELOPMENT)

Figure 4.

SCHEMATIC OF HIGH-TEMPERATURE PANEL-EDGE SEAL RIG (U)

A high temperature panel-edge seal test fixture has recently come on-line at NASA Lewis Research Center. The fixture can measure static seal leakage performance from room temperature up to 1500 °F, and air pressures up to 100 psi (ref. 8). Leakage performance of the seals can be measured while sealing against flat or engine-simulated distorted walls by interchanging the front wall shown. These engine wall distortions can be as large as 0.15 in. in only an 18 in. span.

The Inconel test fixture is heated to the operating condition by high watt-density surface conduction heaters attached to the top and bottom of the rig. Simulated high temperature engine gas is supplied to the rig plenum by electric air heaters. Seal leakage is measured by flow meters upstream of these air heaters. The fixture is designed to evaluate seals 3-ft long, a typical engine panel length. The seal channel can be configured to test square, circular, or rectangular seals that are nominally 0.5 in. high. The sensitivity of leakage performance to lateral or axial loading can also be measured using specially designed high temperature lateral and axial bellows preload systems. Lateral load is applied using a series of high temperature, 0.5 in. diameter Inconel bellows located in the seal channel behind the seals. Load is transferred to the seal by the thin seal backing plate. Axial preload is applied through a hermetically sealed axial bellows/push rod loading system that can apply compressive or tensile loads to the seal over significant stroke lengths without leakage.

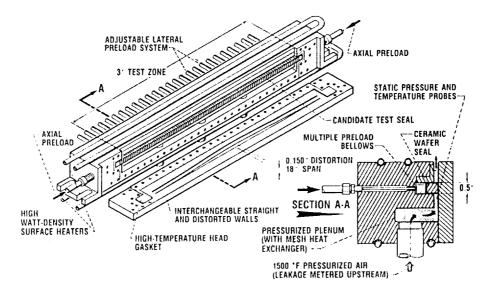# Schematic of High-Temperature Panel-Edge Seal Rig

Figure 5.

NASP HIGH TEMPERATURE TEST FIXTURE (U)

The seal test fixture is shown in this photograph with a ceramic wafer seal installed (note the white horizontal stack of wafers mid-height in the rig). Testing of these linear seals requires special attention be paid to sealing their ends. Leakage around the ends of the seal is minimized using the following approach: over the last inch on the ends of the seal, the face of the fixture, the nose of the wafers, and the face of the front wall all meet in the same plane. Hence, in these two end sections there is no gap to seal. The air follows the path of least resistance and goes through the intended 36 in. center test zone.

Visible on the left and right ends of the fixture are the axial preloader systems mentioned earlier. These preloaders consist of a pneumatic actuator and a calibrated load cell which apply axial loads to the seal through the hermetically sealed bellows push-rod assembly. Below the bench top are the electric air heaters and mass flowmeters. To minimize heat loss and expedite testing, low conductivity insulating board was carefully fit around the entire test fixture.

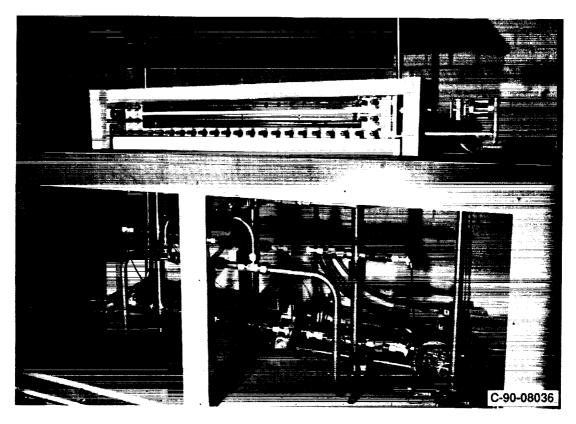## NASP High Temperature Test Fixture

C-90-08036

Figure 6.

ORIGINAL PAGE
BLACK AND WHITE PHOTOGRAPH

SEAL TEST FIXTURE THERMAL EXPANSION (U)

Design of this sizable seal test fixture for high temperature service required attention to be paid to issues not common to conventional design. Thermal growths, for instance, were a particular design issue because of the large temperature rise and large fixture size. The calculated thermal growth of the 40 in. fixture for over a 1400 °F temperature rise was 0.5 in. Ignoring thermal growths of this magnitude often results in excessively high stresses that lead to unforgiving failures. This thermal growth observed during testing was accommodated by slotted feet machined into the rig base.

This thermal expansion also had to be considered when designing the seal axial loading systems. Many of the seal concepts to be tested in this fixture are made of ceramic having a considerably lower coefficient of thermal expansion than the Inconel rig. To accommodate the differential expansion between the rig and the seals, long-stroke hermetically-sealed axial preloaders are used to maintain axial loading on the seal during operation. Differential thermal growth between the Inconel rig and a 3-ft length of Al_2O_3 seal is over 0.25 in.

Seal Test Fixture Thermal Expansion

Figure 7.

CERAMIC WAFER SEAL LEAKAGE TEMPERATURE DEPENDENCE (U)

The high temperature test fixture was used to assess the ceramic wafer seal leakage rates for pressures up to 100 psi and air temperatures up to 1350 °F. Air in the engine reaches this temperature 1 to 2 ft forward of the engine combustor for a Mach 8 (Q = 1500 psf) flight condition. A complete discussion of the test conditions and seal performance results can be found in reference 9. The seal leakage rates shown were measured over the full temperature range for a simulated engine pressure differential of 40 psi. The seal met the industry established tentative leakage limit for all combinations of temperature, pressure and engine wall distortion conditions considered. The seal accommodated and sealed the flat and engine simulated distorted wall conditions equally well.

To assist seal designers in predicting seal leakage flow for the many conditions of pressure and temperature in the engine, leakage flow models have been developed for each seal class. The leakage rates predicted by the wafer seal leakage flow model (see equation in figure) are also plotted and agree well with the measured leakage rates. Details of the seal flow model development may also be found in reference 9. The relevant flow model terms include: the inlet and exhaust pressures, P_s and P_o; gas properties, μ, R, T, film gap heights, h_1 and h_2; seal-to-wall contact dimensions, H_1 and H_2; the number of wafers, N; the inter-panel gap width, g; the seal length, L; and the inter-wafer gap size, h_s. The measured leakage rates being slightly higher than the predicted values can be caused by several factors, including: a small amount of end leakage around the wafers not accounted for in the model; and a possible nonlinear distribution of inter-wafer gaps (e.g., h_s) along the seal length resulting in disproportionate flow between a few wafers.

Ceramic Wafer Seal Leakage Temperature Dependence
40 psi Engine Pressure; Flat Wall

$$\dot{M} = \frac{(P_s^2 - P_o^2)}{24\,\mu RT} \left(\underbrace{\frac{Lh_1^3}{H_1} + \frac{Lh_2^3}{H_2}}_{\substack{\text{Parasitic}\\\text{leakage}\\\text{around}\\\text{wafers}}} + \underbrace{\frac{Ngh_s^3}{H_2}}_{\substack{\text{CTE}\\\text{mismatch}\\\text{Induced}\\\text{leakage}}} \right)$$
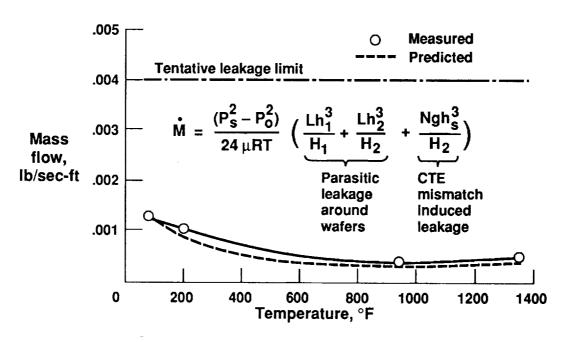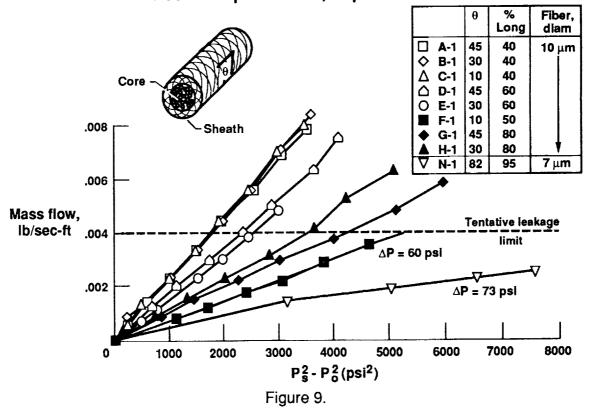
Figure 8.

TWO-DIMENSIONAL BRAIDED ROPE SEAL LEAKAGE PERFORMANCE (U)

A family of eight two-dimensional braided seals were produced and leak tested for engine pressure differentials up to 60 psi. These seals consisted of a core made of uniaxial fibers with a two-dimensional braided sheath or cover to give the seal structural integrity. The room temperature air data shown here are for three percentages (40, 60, 80 percent) of uniaxial or longitudinal fibers and three braiding angles (10°, 30°, 45°). To minimize testing costs E-glass yarns having nominally the same denier (812 denier) and fiber diameter (10 μm) of Nextel yarns were used. The only seal in this 3 by 3 matrix not tested was a seal with an 80 percent longitudinal core and a 10° braid angle which had inadequate structural integrity. Seal specimens were tested at lateral preloads of 80 and 130 psi. The data shown are for 80 psi lateral preload pressure applied by a linear diaphragm along the backside of the seal.

The general data trends indicate that relatively low leakage can be obtained using high percentages of longitudinal fibers, low denier yarns, the smallest diameter fibers possible, and firm lateral preloads. The interaction between surface braid angle and percent longitudinal core is still being investigated. Acceptable braided rope seal leakage rates, as compared to the tentative leakage limit, have been obtained for pressure differentials up to 60 and 80 psi for lateral preload pressures of 80 and 130 psi, respectively. In all test cases presented the seal downstream pressure is atmospheric.

Leakage data were also recently collected for a high density seal denoted N-1. To explore the lower bounds on braid leakage, the seal was braided of small diameter (7μm) carbon fibers using very a high percentage of uniaxial core fiber (95 percent) and very high braiding angle (82°) for the sleeve. As is shown by the lower curve in the figure, the leakage rates are very low and meet the leakage limit for pressure differentials exceeding 70 psi. This seal has offered insight into the beneficial effects of high braid angle that will be further studied during the next phase of this program.

2-D Braided Rope Seal Leakage Performance
Room Temperature Air, 80 psi Preload

		θ	% Long	Fiber, diam
□	A-1	45	40	10 μm
◇	B-1	30	40	
△	C-1	10	40	
◠	D-1	45	60	
○	E-1	30	60	
■	F-1	10	50	
◆	G-1	45	80	
▲	H-1	30	80	
▽	N-1	82	95	7 μm

Figure 9.

BRAIDED ROPE SEAL LEAKAGE:
COMPARISON OF MEASURED AND PREDICTED LEAKAGE RATES (U)

A leakage model for the two-dimensional braided rope seal structures has been formulated. The model treats the seal structure as a system of flow resistances analogous to a series of resistors in an electrical network. For the purposes of this model development, resistance is defined as the ratio of the difference in the squares of the upstream and downstream pressure (e.g., the flow potential) to the mass flow per unit seal length (e.g., the current). This approach allows the fundamental in-homogeneity of the seal's core and sheath to be characterized. Resistances of the fiber bundles are calculated using the Kozeny-Carmen relation where the characteristic size dimension is a scaled fiber diameter (e.g., 0.75 D_f; ref. 10), based on experimental observations.

Measured leakage rates for two different seal architectures (denoted A1 and G1) are plotted here along with the predictions made using the leakage model developed during this program. The predicted leakage rates agree favorably to the measurements for both of these architectures, even though the absolute leakage rates of the two specimens differ by a factor of almost 2.5. The discrepancy noted between the measured and predicted values is generally less than 20 percent for seal A1, and less than 30 percent for seal G1. The sources of these discrepancies can include: some variability in installed and ideal fiber packing densities; data scatter; and some small unavoidable end leakage. These predictions are substantially closer to the measured values than those obtained with the unmodified, homogeneous-porous-media predictions of the Kozeny-Carmen relations, which underestimate leakage rates by more than an order of magnitude. Ongoing model refinements are aimed at minimizing the noted discrepancies and accounting for the effects of seal preload on seal permeability.

Because of the many environments the seals are expected to operate in, it is important to be able to predict the seal leakage flow resistance to various potential engine gases or coolant gases. A series of leakage measurements were run (not shown) for air and helium (a candidate coolant gas with largely different gas transport properties). The results of these experiments confirmed the leakage flow model predictions that the seal leakage flow resistance is directly proportional to viscosity and inversely proportional to the molecular weight of the gas.

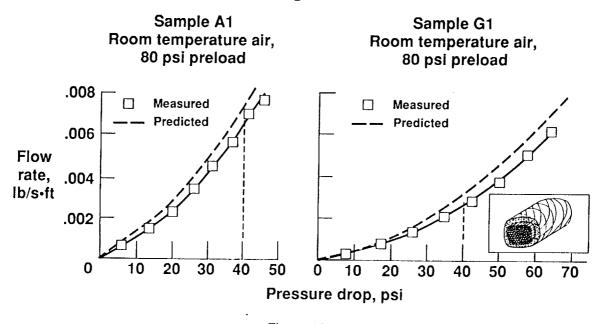## Braided Rope Seal Leakage Measured and Predicted

Figure 10

CERAMIC WAFER SEAL FRICTION RESULTS (U)
EXAMPLE: ENGINE NOZZLE FLAP

Extensive friction and wear experiments for a wide range for candidate seal and engine materials have been performed under engine simulated sliding and temperature conditions (refs. 7 and 11). For the purposes of this paper, a case example will be used to review the typical experimental work performed. In the nozzle section of the NASP vehicle, an articulating flap is being considered to tailor engine flow to optimize engine performance. For this application two types of friction are important should the wafer seal be selected for the nozzle flap: friction between the seal and the nozzle wall; and friction between the adjacent wafers where low friction is required to facilitate inter-wafer sliding to accommodate engine wall distortions.

Data in the left figure is for the first case in which the aluminum oxide seal material is in sliding contact with an Incoloy 909 heat exchanger. Friction coefficients are shown for room temperature and 1200 °F for simulated slow sliding speeds. These measurements were made using a unique high temperature pin-on-disk tribometer at NASA Lewis Research Center (ref. 12). Data shown in the right figure is for the aluminum oxide material sliding against itself simulating inter-wafer sliding. The friction coefficients were quite high at both room temperature and 1600 °F. To lower this friction, a new high temperature solid film lubricant approach has been developed. In this approach lubricous silver was sputtered onto a special titanium bond coat previously sputtered on the ceramic material. The friction coefficient of the lubricated aluminum oxide was 50 percent less than the unlubricated material. Tests are planned to assess the performance of this lubricant at simulated engine temperatures.
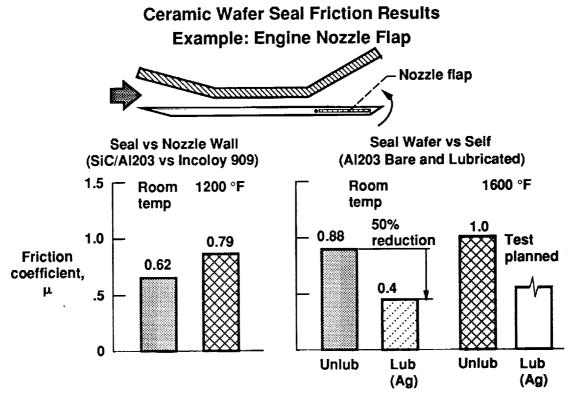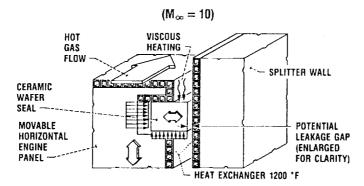

Figure 11.

CERAMIC WAFER SEAL
THERMAL-STRESS ANALYSIS BOUNDARY CONDITIONS ($M_\infty = 10$) (U)

A thermal-structural analysis was conducted of the ceramic wafer seal for several key regions in the engine in reference 4. The important results of that study are reviewed here for the seal mounted in the combustor entrance region where the heating rates under Mach 10 flight are severe and can be as high as 1160 Btu/ft^{2}sec.

Seal thermal boundary conditions for the steady state thermal analyses conducted are indicated below. To maintain the seal temperature below the 2500 °F operating limit of the silicon carbide wafer seal under this intense heating rate, a small flow rate of 70 °F, 15 psi helium was flowed through the small gap between the nose of the seal and the adjacent splitter wall (see ref. 4 for a discussion of estimating the purge flow gap size). An inert gas purge such as helium not only effectively cools the seal but flowing positively into the engine chamber minimizes chances of ingesting potentially explosive unburned hydrogen behind the movable engine panels. The seal temperature distribution shown in the next figure was found using the MARC finite element code run iteratively with a finite difference code to account for the coolant effects of the helium flowing past the seal nose. For the purposes of these analyses a low surface contact conductance of 250 Btu/ft^2 hr °F was used at the interface between the wafer and the seal channel.

Using the temperature distribution determined a structural analysis was performed using the MARC finite element program. For the analyses an 80 psi mechanical preload was applied (with the metal bellows preload system) along the backside of the ceramic wafers and the 15 psi helium pressure differential was applied to the lower surface of the seal in the finite element model. The resulting force urged the seal up and in contact with the top surface of the seal channel. The top interface and the interface between the seal nose and the vertical splitter wall were structurally modelled using gap elements that allowed the wafers to locally expand, move along the adjacent surface and even move away from the surface to accommodate thermal distortions.

Ceramic Wafer Seal
Thermal Stress Analysis Boundary Conditions

($M_\infty = 10$)

THERMAL

VISCOUS HEATING = 1160 Btu/ft^2 s
GAP PURGED WITH 70 °F He GAS
TOP OF SEAL IN CONTACT WITH SEAL CHANNEL:
CONTACT CONDUCTANCE = 250 Btu/ft^2 hr °F

STRUCTURAL

BELLOWS PRELOAD = 80 psi
He PURGE PRESSURE = 15 psi

CD-89-43587

Figure 12.

SEAL TEMPERATURE DISTRIBUTION FOR COMBUSTOR ENTRANCE
HEAT FLUX (U)
(GAP: PURGED WITH HELIUM)

The temperature distribution of the ceramic wafer seal is shown here cooled with 70 °F helium supplied to the base of the seal at a pressure 15 psi above the local flowpath pressure. As the purge gas flows vertically between the nose of the seal and the adjacent sidewall the seal is significantly cooled. The maximum seal temperature found was just under 2300 °F and is at the top of the seal where it is exposed to the maximum heat flux of 1160 Btu/ft^2sec^2. Though the maximum seal temperature was below the 2500 °F operating limit of the silicon carbide wafers, a severe temperature gradient of more than 1000 °F was calculated within the seal. (Note: The temperature of the surrounding heat exchanger structure including the seal channel and splitter wall was cooled to 1200 °F, even if the picture appears slightly different.)
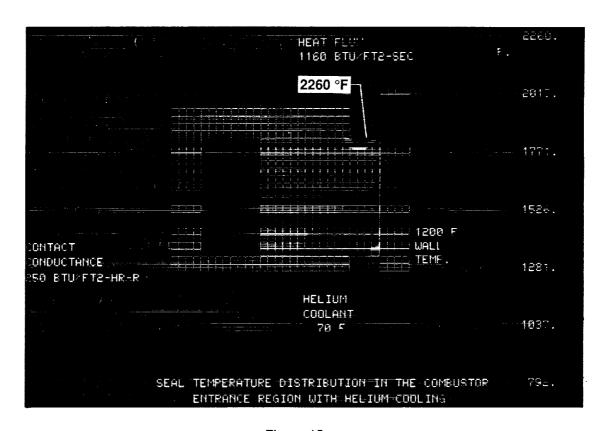

Figure 13.

CERAMIC WAFER SEAL PRINCIPAL STRESSES (U)

For the temperature distribution and the structural boundary conditions described the maximum tensile principal stress found was 24 ksi. The tensile principal stress was examined because typical of ceramics, silicon-carbide is a brittle material that fails in tension.

The silicon-carbide material considered for these analyses was a sintered-alpha silicon carbide (designated SA) made by the Carborundum Corporation.* The tensile strength of this material is very stable with temperature and remains at 35 ksi for temperatures up to 2550 °F, (ref. 13). Studies (ref. 14) have also shown that the flexural strength of this silicone carbide is not effected by hot hydrogen environments. The maximum tensile stress of 24 ksi found along the nose of the seal is roughly two-thirds the tensile strength of the material. The minimum principal stress was also examined and was a small percentage of the silicon carbide's 560 ksi compressive strength.

Based on the steady-state thermal structural analyses performed, the ceramic wafer can withstand the thermal stresses induced. However, recent room temperature leakage tests performed with these silicon carbide wafers have uncovered a potential limitation, (ref. 15). The silicon carbide wafers chipped at their corners during room temperature leakage testing resulting in some additional leakage. Radiography of the seal wafers revealed inclusions and impurities in the wafers that combined with the relatively low fracture toughness of this material were the likely cause of the corner chipping. Efforts to improve the fracture toughness of this material are underway at the manufacturers. However, if these efforts prove unsuccessful, alternate ceramic materials exist that are considerably tougher than silicon carbide. The material trade study performed in reference 15 for instance examined several competing commercially available ceramic materials. For the many properties and materials considered, the material having the best overall balance of properties was a silicon nitride material, Kyocera* SN-251. However, the lower high-temperature conductivity of this material would require higher coolant flow rates to maintain operating temperatures within the material's limit.
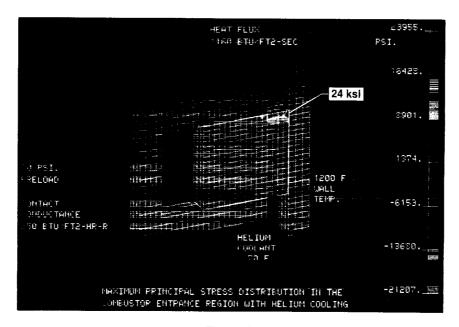

Figure 14.

---

* Trade names or manufacturers' names are used in this report for identification only. This usage does not constitute an official endorsement, either expressed or implied, by the National Aeronautics and Space Administration.

DURABLE BRAIDED ROPE SEAL TECHNOLOGY DEVELOPMENT (U)

Having reviewed some of the major seal accomplishments made during the Technical Maturation Program, some major elements of NASA Lewis Research Centers' NASP Engine Seal Technology Government Work Package (GWP 79) will be highlighted. A major focus of this program will be to develop the seal technology base to demonstrate low-leakage, durable braided-rope seals. An experimental test fixture is under development at NASA Lewis Research Center that will enable assessment of changes in seal leakage due to engine simulated sliding while at temperature and pressure. A success-oriented matrix of solid braided rope seals will be defined based on collective team leakage and durability experience. The main goals of this effort will be: to define seal architectures and materials to achieve the best balance of low-leakage, durable seal operation; and to develop empirical relationships characterizing the interaction between the key variables to be used in future NASP engine seal design efforts. Also key manufacturing technologies such as braid joining will be developed and experimentally assessed.

Durable Braided Rope Seal Technology Development

Objective:

Develop seal technology base and demonstrate low leakage, durable braided-rope seals under engine simulated sliding, pressure, and temperature conditions

Approach:

1. Fabricate and test success-oriented matrix of solid braided rope seals chosen through collective team leakage and durability experience.

2. Develop empirical relationships characterizing interaction of simulated: sliding; pressure; temperature; preload on seal leakage and durability performance.

3. Develop/assess key braiding manufacturing technologies (e.g., braid joining, etc.).

4. Complete information in design guides.

5. Test rigs:
   Hot, dynamic leakage performance rig (NASA; under development)
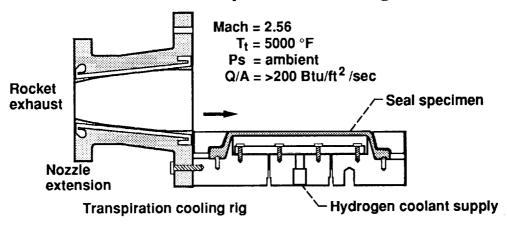   Hot, screening wear rig (P&W MMT rig; operational)

Figure 15.

P&W/NASA TRANSPIRATION COOLING TESTS (U)

The heating rates within the NASP engine are severe ranging up to 1160 Btu/ft^2sec for a Mach 10 flight condition, reference 4. Compounding the seal challenge is the erosive supersonic flow condition present while operating in the SCRAMJET mode. To assess the survivability of the braided rope seal design, P&W and NASA Lewis Research Center have established a cooperative program to test braided rope seal specimens in the exhaust of a hydrogen-oxygen rocket at NASA Lewis. The rocket exhaust is supersonically expanded in the nozzle extension shown. The hot (5000 °F total temperature) gas flows over a 6 in. length of the braided seal held in the horizontal heat-sink copper test fixture shown. Analyses indicate the seal will be subjected to a heat flux of >200 Btu/ft^2sec. No enclosure exists around the seal fixture so surrounding pressure is ambient.

In addition to assessing seal survivability, the tests will also be used to define transpiration cooling effectiveness for various coolant supply conditions. Either nitrogen gas or hydrogen coolant gas will be transpired through the braid. Temperature and coolant flow rate measurements made will be used to determine the seal coolant effectiveness.

P&W/NASA Transpiration Cooling Tests

Figure 16.

ROCKET TEST FACILITY (U)

The rocket test facility to be used for the transpiration seal tests is operational and is shown here during a hot test of a candidate engine cowl-lip. The hydrogen-oxygen rocket typically fires for 3 to 4 sec. Using the supersonic nozzle extension total temperatures up to 5000 °F and stagnation heat fluxes up to 2500 Btu/ft^{2}sec are possible. Complete details of the test capabilities of the facility are found in reference 16.
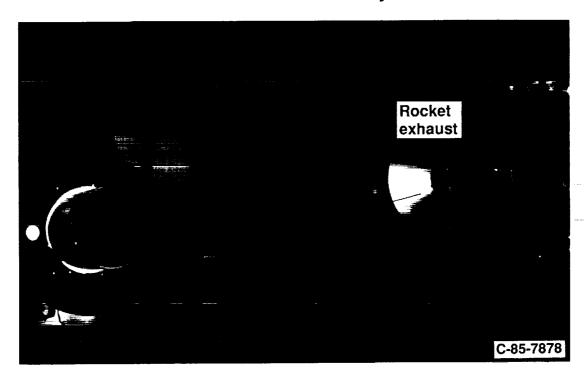
Rocket Test Facility

Figure 17.

SUMMARY AND CONCLUSIONS (U)

Significant progress has been made in maturing and assessing the performance of two classes of NASP engine seals. The ceramic wafer seal has proven effective in minimizing leakage of hot engine gases from room temperature up to 1350 °F over the full range of 0 to 100 psi engine pressure differentials. The ceramic wafer seal meets the tentative leakage limit for all combinations of temperature, pressure, and adjacent wall conditions examined, sealing flat and engine simulated distorted walls equally well. The wafer seal leakage rates were assessed using a static seal test fixture capable of 1500 °F operation installed at NASA Lewis Research Center. This test fixture will play an important role in evaluating candidate seal performances as the NASP project progresses toward the X-30 research vehicle.

Key braiding parameters have been identified for minimizing seal permeability and leakage rates for two-dimensional braided rope seals. Low leakage can be obtained by using: a relatively high percentage of longitudinal fibers; small diameter fibers bundled in low denier yarns; and firm lateral preload. A seal structure made using these design specifications met the tentative leakage limit at room temperature for engine pressure differentials of 60 and 80 psi for lateral preloads of 80 and 130 psi, respectively. Three feet long seals made to these specifications using Nextel fibers are currently being tested in the high temperature test fixture at NASA Lewis Research Center.

Leakage models for each of the ceramic wafers and braided rope seals have been formulated. These models are useful in predicting seal leakage rates for the broad range of engine temperatures and pressures and are being validated using experimental data obtained from room and high temperature test fixtures.

Key results of a detailed thermal-structural analysis performed for the ceramic wafer seal have been reviewed. For the engine inlet and combustor entrance regions considered, thermal stresses found were within the allowable strength limit. Under the intense heating rates of the combustor entrance region a small purge flow of coolant is required to maintain seal temperatures within acceptable limits. Also highlighted were the extensive efforts to assess seal material friction and wear properties under engine simulated temperature and sliding conditions, and to develop innovative solid film lubricants.

Summary and Conclusions

- Ceramic wafer seal performance assessed at temperatures up to 1350 °F and at pressures up to 100 psi. Seal performed well meeting the tentative leakage limit for both flat and engine simulated distorted wall conditions.

- Key braided rope seal parameters limiting leakage identified. Low leakage braided rope seals tested that meet tentative leakage limit for pressures up to 60-80 psi depending on preload.

- Leakage models for each class of seal developed. Model validation nearly complete.

- Thermal-structural analyses of SiC ceramic wafer seal under high heat flux conditions performed: Thermal stresses within allowable strength limit.

- Friction coefficients of candidate seal materials measured over a wide temperature range. Solid lubricants developed and under evaluation.

Figure 18.

SEAL TECHNOLOGY DEVELOPMENT PLANS (U)

Several of the seal technology development tasks underway within Government Work Package 79 have been reviewed. To address issues raised in the seal design critiques, NASA is developing a test capability to enable assessment of braided-seal flow rate change over simulated engine sliding distances while at temperature and pressure. A matrix approach will be pursued that will be used to identify seal architectures and materials for the best balance of low-leakage, durable seal performance. Durability of alternate candidate fibers and coatings will be also assessed early to positively influence fiber material selection.

A cooperative P&W/NASA Lewis Research Center program has been established to assess braided rope seal survivability and cooling effectiveness in the supersonic, high heat flux environment typical of the NASP engine. Candidate braided rope seals will be subjected to heat fluxes >200 Btu/ft^2 sec in a Mach 2.56 rocket exhaust flow using NASA Lewis Research Centers' Hot Gas Facility.

Seal Technology Development Plans

- **Aggressive program to develop durable braided rope seals and seal technology: Required test-hardware design underway.**

- **Experimental program to assess alternate ceramic fiber durability: Underway.**

- **P&W/NASA hot gas tests to assess seal survivability and define coolant effectiveness under engine simulated heating rates.**

Figure 19.

REFERENCES

1. Steinetz, B.M.; DellaCorte, C.; and Sirocky, P.J.: On the Development of Hypersonic Engine Seals. NASA TP-2854, 1988.

2. Sawko, P.M.; and Tran, H.K.: Strength and Flexibility Properties of Advanced Ceramic Fabrics. SAMPE Q., vol. 17, no. 1, Oct. 1985, pp. 7-13.

3. Steinetz, B.M.; DellaCorte, C.; and Tong, M.: Seal Concept and Material Performance Evaluation for the NASP Engine. NASA CP-7045, Vol. VI-Structures, 1989, pp. 39-58.

4. Tong, M.; and Steinetz, B.M.: Thermal and Structural Assessments of a Ceramic Wafer Seal in Hypersonic Engines. AIAA Paper 91-2494, June 1991. (Also, NASA TM-103651.)

5. DellaCorte, C.; and Sliney, H.E.: Composition Optimization of Self-Lubricated Chromium-Carbide-Based Composite Coatings for Use to 760 °C. ASLE Trans., vol. 30, no. 1, Jan. 1986, pp. 77-83.

6. Eckel, A., et al.: Thermal Shock of Fiber Reinforced Ceramic Matrix Composites. NASA TM-103777, 1991.

7. Dursch, H.W., et al: National Aerospace Plane (NASP) Airframe Technology Option Five: Sealing Concepts. Air Force Contract No. F33657-86-C-0061, Boeing Advanced Systems, July 21, 1989.

8. Steinetz, B.M.: A Test Fixture for Measuring High-Temperature Hypersonic Engine Seal Performance. NASA TM-103658, 1990.

9. Steinetz, B.M.: High Temperature Performance Evaluation of a Hypersonic Engine Ceramic Wafer Seal. NASA TM-103737, 1991.

10. Tao, X., et al.: Development of Improved Hypersonic Engine Seals: Part II, Flow Modelling. AIAA Paper 91-2495, June, 1991 (Also, NASA TM-104371, 1991).

11. DellaCorte, C.; Steinetz, B.M.; and Brindley, P.K.: Tribological Properties of Ceramic/Ti3Al-Nb Sliding Couples for Use as Candidate Seal Materials to 700 °C. NASA TM-102401.

12. Sliney, H.E.; and DellaCorte, C.: A New Test Machine for Measuring Friction and Wear in Controlled Atmospheres to 1200 °C. NASA TM-102405, 1990.

13. Hecht, N.: Mechanical Properties Characterization of High Performance Ceramics. 27th Automotive Technology Development Contractors Coordination Meeting. Society of Automotive Engineers, 1990. (To be published in Ceram. Eng. Sci. Proc., vol. 12, no. 7-8, 1991.)

14. Herbell, T.P., et al.: Effect of Hydrogen on the Strength and Microstructure of Selected Ceramics. NASA TM-103674, 1990.

15. Steinetz, B.M.: Evaluation and Ranking of Candidate Ceramic Wafer Engine Seal Materials. NASA TM-103795, 1991.

16. Melis, M.E., et al.: A Unique Interdisciplinary Research Effort to Support Cowl Lip Technology Development for Hypersonic Applications. NASA TP-2876, 1989.

NASA
National Aeronautics and
Space Administration

Report Documentation Page

1. Report No.	2. Government Accession No.	3. Recipient's Catalog No.
NASA TM-104468		

4. Title and Subtitle		5. Report Date
High Temperature NASP Engine Seals A Technology Review		
		6. Performing Organization Code

7. Author(s)	8. Performing Organization Report No.
Bruce M. Steinetz, Christopher DellaCorte, and Mike Tong	E-6317
	10. Work Unit No. 763-21-41

9. Performing Organization Name and Address	11. Contract or Grant No.
National Aeronautics and Space Administration Lewis Research Center Cleveland, Ohio 44135-3191	
	13. Type of Report and Period Covered Technical Memorandum

12. Sponsoring Agency Name and Address	14. Sponsoring Agency Code
National Aeronautics and Space Administration Washington, D.C. 20546-0001	

16. Abstract

Progress in developing advanced high temperature engine seal concepts and related sealing technologies for advanced hypersonic engines are reviewed. Design attributes and issues requiring further development for both the ceramic wafer seal and the braided ceramic rope seal are examined. Leakage data are presented for these seals for engine simulated pressure and temperature conditions and compared to a target leakage limit. Basic elements of leakage flow models to predict leakage rates for each of these seals over the wide range of pressure and temperature conditions anticipated in the engine are also presented. The paper concludes with an outline of a seal development program to address the seal technology issues raised during the Technical Maturation Phase of the National Aerospace Plane Program.

17. Key Words (Suggested by Author(s))	18. Distribution Statement
Seals High temperature Lubrication Hypersonic engine	Unclassified - Unlimited Subject Category 37

19. Security Classif. (of the report)	20. Security Classif. (of this page)	21. No. of pages	22. Price*
Unclassified	Unclassified	24	A03